PROTEINS
STRUCTURE ■ FUNCTION ■ BIOINFORMATICS

Deformability in the cleavage site of primary microRNA is not sensed by the double-stranded RNA binding domains in the microprocessor component DGCR8

Kaycee A. Quarles, Durga Chadalavada, and Scott A. Showalter*

Department of Chemistry, Center for RNA Molecular Biology, The Pennsylvania State University, University Park, Pennsylvannia 16802

ABSTRACT

The prevalence of double-stranded RNA (dsRNA) in eukaryotic cells has only recently been appreciated. Of interest here, RNA silencing begins with dsRNA substrates that are bound by the dsRNA-binding domains (dsRBDs) of their processing proteins. Specifically, processing of microRNA (miRNA) in the nucleus minimally requires the enzyme Drosha and its dsRBD-containing cofactor protein, DGCR8. The smallest recombinant construct of DGCR8 that is sufficient for *in vitro* dsRNA binding, referred to as DGCR8-Core, consists of its two dsRBDs and a C-terminal tail. As dsRBDs rarely recognize the nucleotide sequence of dsRNA, it is reasonable to hypothesize that DGCR8 function is dependent on the recognition of specific structural features in the miRNA precursor. Previously, we demonstrated that noncanonical structural elements that promote RNA flexibility within the stem of miRNA precursors are necessary for efficient *in vitro* cleavage by reconstituted Microprocessor complexes. Here, we combine gel shift assays with *in vitro* processing assays to demonstrate that neither the N-terminal dsRBD of DGCR8 in isolation nor the DGCR8-Core construct is sensitive to the presence of noncanonical structural elements within the stem of miRNA precursors, or to single-stranded segments flanking the stem. Extending DGCR8-Core to include an N-terminal heme-binding region does not change our conclusions. Thus, our data suggest that although the DGCR8-Core region is necessary for dsRNA binding and recruitment to the Microprocessor, it is not sufficient to establish the previously observed connection between RNA flexibility and processing efficiency.

Proteins 2015; 83:1165–1179.

Key words: RNA interference; protein interactions; dsRNA; microRNA; dsRBD; DGCR8; Drosha; binding affinity; in vitro processing; heme binding domain.

INTRODUCTION

One of the most significant recent breakthroughs in biology, especially for the therapeutic community,[1,2] has been the discovery of RNA interference (RNAi), which is involved in a wide range of developmental, immunity, and regulatory networks.[3,4] As part of RNAi, the canonical microRNA (miRNA) maturation pathway includes a series of steps beginning in the nucleus with cleavage by the Microprocessor complex, progressing to the cytoplasm with cleavage by Dicer, and ending with incorporation into the RNA-induced silencing complex.[5] Despite the centrality of this pathway to the eukaryotic gene regulation program, much is still unknown about the molecular mechanism of miRNA processing. Specifically, the complexity of RNA structure in cellular pools and the prevalence of double-stranded RNA (dsRNA) are both far more pronounced than previously appreciated.[6–8] Improper substrate recognition within the miRNA maturation pathway can result in the accumulation of unprocessed miRNAs and/or misregulated mRNA levels, culminating in a multitude of clinical effects.[9] Therefore, miRNA processing proteins face a crucial, complex task in selecting primary miRNA (pri-miRNA) targets from a pool of diverse dsRNA structures. For these reasons, gaining mechanistic insight into the molecular-scale rules for RNA selection by miRNA processing complexes remains a high priority.

Additional Supporting Information may be found in the online version of this article.

Grant sponsor: US National Institutes of Health; Grant number: R01GM098451.
*Correspondence to: Scott A. Showalter, Department of Chemistry and Center for RNA Molecular Biology, The Pennsylvania State University, 104 Chemistry Building, University Park, PA 16802. E-mail: sas76@psu.edu
Received 18 September 2014; Revised 10 March 2015; Accepted 25 March 2015
Published online 7 April 2015 in Wiley Online Library (wileyonlinelibrary.com).
DOI: 10.1002/prot.24810

Wherever dsRNA is encountered, the dsRNA-binding domain (dsRBD) is typically employed for the binding of dsRNA.[10,11] In the canonical metazoan miRNA maturation pathway, there are five key proteins that contain dsRBDs: DGCR8, Drosha, TRBP, PACT, and Dicer. In this study, we focus on the pair of dsRBDs found in the Microprocessor component DGCR8, which is involved in the initial stage of miRNA processing. At the level of amino acid sequence, the RNA-binding face of a given dsRBD motif is typically evolutionarily conserved across species although this conservation does not generally extend across orthologous dsRBD-containing proteins.[12] For example, DGCR8 contains two dsRBDs that share only 25% of sequence identity with one another although the sequences of each domain are 98% conserved among mammals. The 3D fold of the dsRBD is structurally similar to the fold of the single-stranded RNA recognition motif (RRM), featuring a mixed α/β topology arranged in the tertiary structure to produce α-helical- and β-sheet-rich faces, but the binding mode observed for dsRBDs is mechanistically distinct from that of RRMs.[13] The structures of dsRBDs bound to dsRNA reveal that the α-helical face of the domain engages the dsRNA through predominantly electrostatic interactions that are nearly always insensitive to the nucleotide sequence of the RNA;[14–18] although exceptions have been noted.[19] This tendency of dsRBDs to bind dsRNA without sequence specificity suggests that proteins like DGCR8 must recognize specific structural features in their RNA targets for function.

It is widely believed that structural features common to pri-miRNAs, but rare in nontarget RNAs, are a key determinant for the recognition by the Microprocessor complex and for resulting high processing efficiency. The typical pri-miRNA contains a long dsRNA stem in the context of a hairpin loop structure, disrupted by multiple noncanonical structural features (i.e., loops and bulges), and adjoined to flanking regions with strong single-stranded character.[20–23] Previously, we have shown that disorder-promoting noncanonical structural elements within the stem of pri-miRNAs are necessary for efficient *in vitro* cleavage by reconstituted Microprocessor complexes.[24] The likely origin of these pri-miRNA structural requirements is in the RNA-binding function of DGCR8, which motivates detailed biochemical characterization of this key dsRNA-binding protein.

Interestingly, although the enzymes Dicer and Drosha each contain a single dsRBD, their cofactor proteins, including DGCR8, each contain multiple dsRBDs, suggesting that these cofactors may gain a functional advantage by arranging multiple dsRBDs in a single polypeptide chain. The most thoroughly studied fragment of DGCR8 that is sufficient for *in vitro* dsRNA binding, referred to as DGCR8-Core, consists only of its two dsRBDs and a short C-terminal tail, which contains an α-helix that the two dsRBDs pack against.[25]

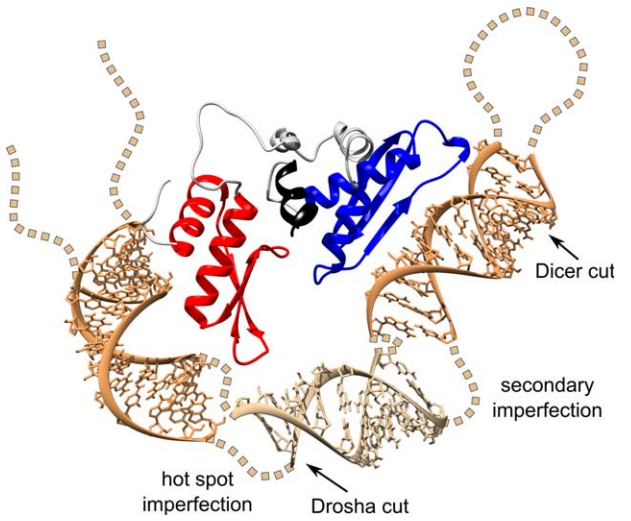

Figure 1

Bending model for pri-miRNA recognition by DGCR8-Core currently supported in the literature.[25] The DGCR8-Core crystal structure (PDB 2YT4, with loops built-in as described previously[26]) is shown with dsRBD1 in red and dsRBD2 in blue. Approximately, one turn of idealized A-form dsRNA (tan) has been modeled in contact with each dsRNA-binding face of DGCR8, with an additional turn of dsRNA shown in between to bridge the space separating the dsRBDs. The flanking tails, flexible regions in the stem, and terminal loop are implied by dotted lines to suggest the full make-up of a pri-miRNA bound to DGCR8-Core. This model suggests that the pri-miRNA must undergo extreme bending to accommodate binding by DGCR8, which may occur at the hot spot and secondary imperfection sites (labeled). Approximate Drosha and Dicer cut sites are also labeled.

Intriguingly, the spatial arrangement of the two dsRBDs within DGCR8-Core is incompatible with their simultaneous binding to pri-miRNA, unless the stem of the pri-miRNA undergoes substantial bending (Fig. 1)[25]; otherwise, DGCR8-Core must undergo a (possibly RNA dependent) global conformational transition. Supporting the possibility of structural rearrangement within DGCR8-Core, molecular dynamic calculations performed by our group lead to the hypothesis that correlated bending about the pseudo-twofold symmetry axis running through the interface between the two dsRBDs induces a conformational change that may facilitate pri-miRNA binding.[26] Recent experimental evidence to support this hypothesis was provided by NMR lineshape analysis, which revealed a substantial change to the chemical environment for the RNA-binding face of both dsRBDs, accompanied by the changes in environment spanning the interface formed between the domains, in the context of RNA-bound DGCR8-Core.[27] Taken together, these observations suggest that DGCR8-Core must undergo some degree of structural rearrangement, even in a binding mechanism featuring strong bending of the stem of pri-miRNA.

In a previous study,[24] we demonstrated a need for flexibility within the pri-miRNA stem for efficient

cleavage by Drosha, but attribution of this result to a measurable impact on dsRNA binding by DGCR8-Core was not attempted. Additional study by others has demonstrated a need for flanking single-stranded RNA and for a large, flexible terminal loop on the hairpin[21,28]; similarly, these studies did not aim to demonstrate that the effects observed were directly DGCR8 mediated. In this study, we focus on DGCR8's interactions with a variety of dsRNAs that contain features commonly found in native pri-miRNA substrates (i.e., ssRNA–dsRNA junction, dsRNA stem, imperfections within the stem, and the terminal loop). Our results show that neither the N-terminal dsRBD of DGCR8 in isolation nor the DGCR8-Core construct is sensitive to the presence of noncanonical structural elements within the stem of pri-miRNA, or to the composition of the RNA flanking the stem. Significantly, we show that periodic (i.e., once-per-turn) flexibility along the RNA stem is not necessary for high-affinity DGCR8-Core binding, which suggests that the strong RNA-bending model may be inaccurate. Furthermore, extending DGCR8-Core to include the N-terminal heme-binding region does not affect RNA binding affinity to our dsRNA constructs, in contrast with the recent literature. Consistent with the rest of our findings, inclusion of the heme-binding region also does not confer novel RNA-structure specificity to DGCR8. To summarize, our data suggest that although the DGCR8-Core region is necessary for RNA binding and recruitment to the Microprocessor, it is not sufficient to establish the previously observed connection between RNA flexibility and processing efficiency.

MATERIALS AND METHODS

Protein preparation

A synthetic DGCR8-Core (505–720) gene was purchased from Geneart, and DGCR8-dsRBD1 (505–583) was amplified by PCR. The expression and purification of the protein was performed as described previously.[29] The protein was buffer exchanged into 50 m*M* cacodylate (pH = 6.0), 50 m*M* KCl, and 0.35 μg/mL β-mercaptoethanol. Final concentration of the sample was determined via guanidine hydrochloride denaturation by UV absorption using $\varepsilon = 22{,}400\ M^{-1}\ cm^{-1}$ (DGCR8-Core) and $\varepsilon = 4200\ M^{-1}\ cm^{-1}$ (DGCR8-dsRBD1), both at 278 nm.

The DGCR8-HBD-Core construct (276–720) was prepared by amplifying DNA through PCR from the human DGCR8 gene, purchased from ATCC, which was then inserted into pET24 vector. Following similar expression and purification protocols as for the other DGCR8 constructs, but without 3C protease cleavage of the his-tag, the recombinant protein was buffer exchanged into 50 m*M* sodium cacodylate (pH = 6.0), 50 m*M* KCl, 0.35 μg/mL β-mercaptoethanol, and 5% v/v glycerol. Final concentration of the sample was determined via guanidine hydrochloride denaturation followed by UV absorption measurement, using $\varepsilon = 44{,}800\ M^{-1}\ cm^{-1}$ at 278 nm.

Primary miRNA preparation

All DNAs containing a pri-miRNA sequence were purchased from Geneart and contained a T7 promoter sequence at the 5′-end, as well as an inverted BsaI cut site at the 3′-end. The preparation of the template DNA, transcription by T7 RNA polymerase, and purification of the transcribed RNA were all performed as described previously.[24]

5′-end labeling of RNA

All RNAs were 5′-end labeled with ^{32}P. To remove the 5′-triphosphate, the RNA was first treated with calf intestinal alkaline phosphatase (New England Biolabs), phenol/chloroform extracted, and ethanol precipitated. The RNA was then 5′-end labeled with T4 polynucleotide kinase (New England Biolabs). The concentration of labeled RNA was determined using a liquid scintillation counter (Beckman).

Native gel RNA purification

For the RNA duplexes, 5′-^{32}P-end-labeled top strand RNA was mixed with 20-fold excess unlabeled bottom-strand RNA (RNAs ordered from Dharmacon) and the electrophoretic mobility shift assay (EMSA) 5× buffer to a final concentration of 20% v/v (Supporting Information Methods: Electrophoretic Mobility Shift Assay Methods). In the case of the duplexes containing terminal loops, the 5′-^{32}P-end-labeled RNA was mixed with the EMSA 5× buffer to a final concentration of 20% v/v. The mixture was denatured at 85 °C for 3 min followed by renaturing at 1 °C for 5 min. Subsequently, the RNA mixtures were run on a 0.25× Tris-borate (TBE), 10% of acrylamide gel at 12 V cm^{-1} at 4 °C for 4 h. The gel was then exposed on film for 30 min and the developed film was used to cut out the corresponding duplex or monomer terminal loop bands from the gel. The gel pieces were soaked overnight at 4 °C in a TEN250 solution, and the RNA was then purified from the supernatant by ethanol precipitation. The concentration of labeled RNA was determined using a liquid scintillation counter (Beckman).

Electrophoretic mobility shift assays

For reactions involving pri-miRNA constructs, the 5′-^{32}P-end-labeled RNA was renatured immediately prior to use by heating to 85 °C for 3 min followed by renaturing at 1 °C for 5 min. Prior to mixing with protein, the binding reactions were incubated at room

temperature for 30 min to ensure full equilibration in the presence of 50 m*M* of cacodylate (pH = 6.0), 50 m*M* of KCl, 5% of glycerol, 100 μg/mL of bovine serum albumin, 1 m*M* of dithiothreitol, and 0.1 mg/mL of herring sperm DNA (to prevent the complex from sticking in the wells). Subsequently, the binding reactions were run on a 0.25× TBE, 10% of acrylamide gel at 12 V cm^{-1} at 4 °C for 3 h, with each lane containing 20 μCi. Signal from the gels was quantified on a Typhoon-9410 imager, and the resulting images were processed in ImageQuant. The fraction bound was calculated as the intensity of all protein-bound species over the sum of the protein-bound species and the free RNA. A more detailed protocol is described in the Supporting Information Methods.

Drosha processing and competition processing assays

RNA substrates for *in vitro* assays were transcribed as described previously.[30] FLAG-Drosha[30] and FLAG-DGCR8 (AddGene) (collectively referred to as Microprocessor) were overexpressed in HEK-293T cells and FLAG-tagged proteins were isolated on M2-FLAG beads (Sigma) as described previously.[24] Lysate (whole cell or immunopurified Microprocessor) was combined with 10 fmol of labeled RNA, 10× reaction buffer (64 m*M* $MgCl_2$), RNasin (Promega), and with (competition processing) or without (regular processing) increasing amounts of purified competitor duplex RNA. The reaction mix was incubated at 37 °C for 15 min. The products were phenol/chloroform extracted and ethanol precipitated, and labeled RNA analyzed on 12% of denaturing PAGE gels. Signal from the gels was quantified on a Typhoon-9410 imager, and the resulting images were processed in ImageQuant. The percent processed was calculated as the intensity of all cleaved species (pre-miRNA and cleaved single-stranded tails) over the sum of all species (cleaved species and substrate pri-miRNA).

RESULTS

Native pri-miRNA substrates for DGCR8 are long (>80 nucleotides) hairpin RNAs, characterized structurally by multiple base-pairing imperfections in their ~30 base-pair stems, a terminal loop, and an unpaired flanking region (termed the ssRNA–dsRNA junction throughout this article). Multiple investigators have studied the prevalence and significance of base-pairing imperfections within the double-stranded stem of the pri-miRNA, leading to the identification of two broadly conserved features: the region located near the Drosha cleavage site (referred to here as the "hot spot")[24]; and the secondary imperfection, located approximately halfway between the Drosha and the Dicer cleavage sites (Fig. 1).[23,31] Although it is widely accepted that an ssRNA–dsRNA junction is necessary for Drosha processing, it is still disputed whether a large, flexible terminal loop is required.[21,32,33] Motivated by the need to clarify the relative importance of each of these pri-miRNA structural features for efficient miRNA processing, we chose to begin this study with an investigation of DGCR8-Core's ability to recognize each of these structural elements in controlled *in vitro* binding reactions.

Binding to pri-miRNAs

The recognition of pri-miRNA by the tandem-dsRBD containing DGCR8-Core has been previously investigated by EMSAs, suggesting that nonspecific association between DGCR8-Core and pri-miRNA is characterized by an apparent dissociation constant ($K_{d,app}$) of ~2 μ*M*, under a range of binding conditions.[25,27,29] Alternatively, the single N-terminal dsRBD from DGCR8 (DGCR8–dsRBD1) binds pri-miRNA with $K_{d,app}$ of ~9 μ*M*,[29] whereas binding by the C-terminal dsRBD (DGCR8–dsRBD2) alone has not been reported owing to limited solubility of this domain in isolation. It is noteworthy that Drosha also contains a dsRBD, but it has not demonstrated the dsRNA-binding activity (Supporting Information Fig. S1). Under solution conditions exactly matching those used throughout this study, we selected the panel of pri-miRNA molecules shown in Figure 2(A) for EMSA analysis to establish the affinities of DGCR8-Core and DGCR8–dsRBD1. The representative gels for DGCR8-Core and DGCR8–dsRBD1-binding assays are shown in Supporting Information Figures S2 and S3, respectively. The investigation of binding using filter binding assays was also attempted, but rapidly abandoned because the binding intermediates appeared not to be sufficiently stable for retention on the membranes, leading to systematic errors in the apparent dissociation constants (Supporting Information Fig. S4). The inspection of the apparent dissociation constants in Table I reveals that although the secondary structures of these three pri-miRNAs vary significantly within the stem region, the affinity of DGCR8-Core for all three is nearly invariant ($K_{d,app}$ range, 1–2 μ*M*). Interestingly, the affinity of DGCR8-Core for the Drosha cleavage product pre-mir-16-1 is also indistinguishable from its measured affinity for any of the three pri-miRNAs employed in the study. In contrast, DGCR8–dsRBD1 displays an approximate threefold variation in affinity among these three pri-miRNA molecules, but binds all three approximately threefold more weakly than DGCR8-Core interacting with the same pri-miRNAs.

Binding to perfect Watson–Crick duplexes

The relatively uniform dissociation constants measured in our pri-miRNA-binding studies suggested that either DGCR8-Core is not sensitive to variations in the structural features of pri-miRNA targets, or that the

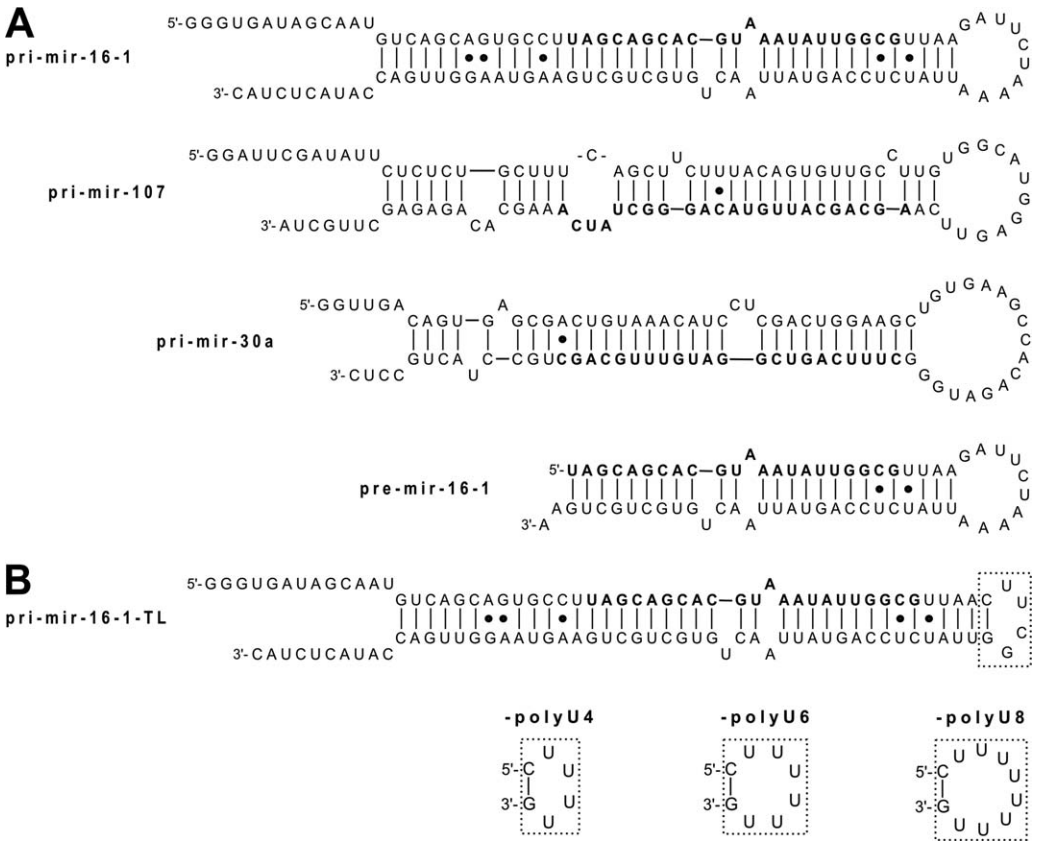

Figure 2

Secondary structures of *in vitro*-transcribed RNA models for (**A**) native pri-miRNAs and pre-mir-16-1; and (**B**) non-native pri-mir-16-1 stem-loop constructs (region of mutation boxed). Secondary structures shown are as predicted experimentally by combined SHAPE/MC-Pipeline analysis.[24] For all constructs, the mature miRNA is indicated in bold.

complexity of their structures masks DGCR8-Core's sensitivity to the presence of individual structural elements. Therefore, we designed a series of model RNA constructs to continue our binding studies that will provide unambiguous assessment of DGCR8-Core's sensitivity to specific structural features. As a baseline for this study, we first characterized DGCR8's ability to bind perfect Watson–Crick (WC) RNA duplexes, with lengths increasing from 12 through 44 bp (Fig. 3, secondary structures). The lengths of WC–dsRNAs used in this study were as follows: (1) 12 bp (ds12), representing the smallest binding site size of a single dsRBD[14,15,17,19,34]; (2) 16 bp (ds16), representing the smallest binding footprint seen

Table I

EMSA Best-Fit Parameters for DGCR8-Core and DGCR8-dsRBD1 Binding to the Native pri- and pre-miRNA Constructs, with Uncertainties Based on Two Independent Replicates

	DGCR8-Core		DGCR8–dsRBD1	
RNA construct	K_d (μM)	n	K_d (μM)	n
pri-mir-16-1	1.05 ± 0.03	3.9 ± 0.4	9.7 ± 0.6	2.3 ± 0.1
pri-mir-107	1.50 ± 0.07	6 ± 1	6.6 ± 0.4	2.3 ± 0.2
pri-mir-30a	1.86 ± 0.09	5.6 ± 0.3	16.7 ± 0.1	1.49 ± 0.01
pre-mir-16-1	1.70 ± 0.09	6.0 ± 0.4	N/D[a]	

[a]N/D, binding not determined/tested.

Figure 3

Secondary structures of perfect WC duplexes derived from pri-mir-16-1 (which is displayed at the top for reference). The mature miRNA strand is shown in bold and the dotted line indicates where each construct's sequence aligns relative to pri-mir-16-1; these are consistent for all RNA model constructs throughout.

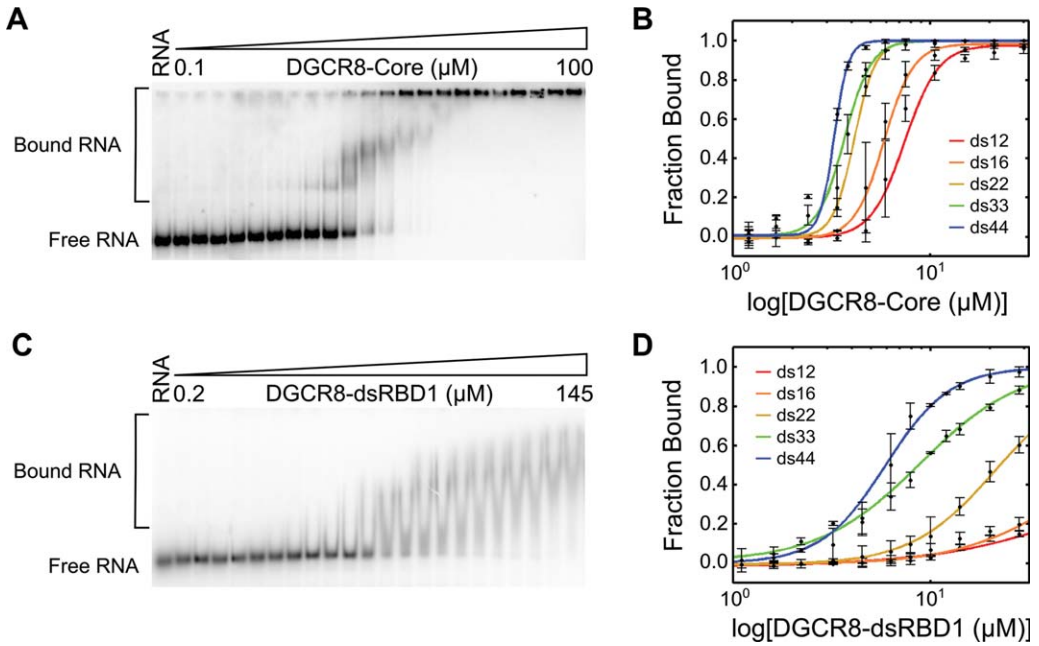

Figure 4

EMSAs used to examine binding by DGCR8 to varying lengths of perfect WC RNA duplexes. Representative gels are shown for both (**A**) DGCR8-Core and (**C**) DGCR8–dsRBD1 binding to ds44. The leftmost lane in the gels contains RNA, but no protein (labeled "RNA" above the gel). In all other lanes, the concentration of protein increases from left to right (triangle above gel). Bands corresponding to free and bound RNA are indicated to the left of the gels. (**B**, **D**) The corresponding fits to the EMSA data for all lengths of duplex (for best-fit parameters, see Table II; fitting procedure is described in the Materials and Methods section). Representative gels for all dsRNA lengths contributing to (B and D) are shown in Supporting Information Figures S5 and S6.

for a tandem dsRBD construct (i.e., proteins similar to DGCR8-Core)[35]; (3) 22 bp (ds22), representing the length of a miRNA:miRNA* duplex; (4) 33 bp (ds33), representing the approximate length of a pre-miRNA; and (5) 44 bp (ds44), representing the approximate length of a pri-miRNA. It is worth noting that, with the exception of the additional sampling created by the ds16 construct, all duplexes differed in length by approximately one turn of A-form RNA duplex, which allows for the examination of binding on a per-helical turn basis.

EMSAs were performed in which either DGCR8-Core or DGCR8–dsRBD1 was titrated into each of the RNA duplexes described above. The representative gels are shown in Figure 4(A,C) for binding to ds44, with representative gels for DGCR8-Core and DGCR8–dsRBD1 binding to all duplexes shown in Supporting Information Figures S5 and S6, respectively. As the length of the RNA duplex increased, the affinity of DGCR8-Core for the duplex also increased modestly, from $K_{d,app} = 8$ μ*M* for binding to ds12 to $K_{d,app} = 3$ μ*M* for binding to ds44 (Fig. 4(B); best-fit parameters in Table II). It should be noted that at high DGCR8-Core concentrations, particularly for titrations into the longer RNA duplexes, high-molecular-weight complexes began to stick in the wells of the gel, which may have been the result of high stoichiometry in the complexes[36] or of DGCR8 self-assembly.[37] In contrast, DGCR8–dsRBD1 shows a much larger change in affinity as RNA duplex length increases, ranging from $K_{d,app}$ of 200 up to 6 μ*M* as the duplex length increases from 12 to 44 bp (Fig. 4(D); best-fit parameters in Table II). It should be noted that the saturation of the binding event was not possible for DGCR8–dsRBD1 binding to ds12 or ds16 owing to the limitations in the solubility of the protein, and hence the reported dissociation constants for these two RNAs should be interpreted as lower limits. In summary, the data from this study of interactions between DGCR8-Core and DGCR8–dsRBD1 with WC RNA duplexes suggest that juxtaposing two dsRBDs in a single polypeptide largely eliminates DGCR8's sensitivity to duplex length for RNAs with lengths similar to Microprocessor substrates and products.

The previous studies have shown that DGCR8-binding affinities correlate well with Drosha-processing efficiencies[21] and that Drosha cleaves remarkably efficiently when in complex with the RNA-binding region of DGCR8 (amino acids 484–750 of the human sequence, which includes the "Core" region).[38] These findings suggest that the trends in dsRNA-binding affinity we observed in our EMSAs should be predictive of the efficiency with which our dsRNA duplexes will inhibit pri-

Table II
EMSA Best-Fit Parameters for DGCR8-Core and DGCR8–dsRBD1 Binding to the Indicated Duplexed RNA Constructs, with Uncertainties Based on Two Independent Replicates

	DGCR8-Core		DGCR8-dsRBD1	
RNA construct	K_d (μ*M*)	*n*	K_d (μ*M*)	*n*
ds12	7.4 ± 0.9	5 ± 2	>200	~1
ds16	5.8 ± 0.8	6 ± 1	>90	~1
ds22	4.1 ± 0.5	8 ± 2	21 ± 1	2.1 ± 0.2
ds33	3.7 ± 0.3	6 ± 2	8.8 ± 0.2	1.7 ± 0.1
ds44	3.3 ± 0.2	12.1 ± 0.7	5.9 ± 0.1	2.66 ± 0.09
ds16 + native flanking	3.41 ± 0.06	5.7 ± 0.2	>25	~1
ds16 + non-native flanking	4.9 ± 0.2	4.3 ± 0.2	>35	~1
ds16 + flanking TS	4.5 ± 0.7	5 ± 1	>55	~1
ds16 + native flanking BS	4.3 ± 0.6	4.8 ± 0.7	>125	~1
ds16 + non-native flanking BS	4.3 ± 0.2	4.0 ± 0.2	>50	~1
16TS	20 ± 2	2.09 ± 0.06	N/B[a]	
ds16 + TL	6.0 ± 0.1	6 ± 1	>90	~1
ds16 + polyU4	6.4 ± 0.2	6.2 ± 0.3	N/D[b]	
ds16 + polyU6	6.4 ± 0.2	4.1 ± 0.1	N/D	
ds16 + polyU8	4.9 ± 0.3	3.8 ± 0.4	>65	~1
HS duplex	4.76 ± 0.02	2.26 ± 0.01	N/D	
miR:miR*	4.67 ± 0.01	2.26 ± 0.01	N/D	
dsAmis	2.35 ± 0.05	3.67 ± 0.08	N/D	
dsUbulge	6.4 ± 0.1	4.3 ± 0.1	N/D	

[a]N/B, no binding was seen between 16TS and DGCR8-dsRBD1.
[b]N/D, binding not determined/tested.

miRNA cleavage by the Microprocessor in a standard *in vitro* RNA-processing assay. Therefore, in an effort to corroborate the trends we observed for DGCR8 affinity to bind RNAs of varying lengths in a more biological context, we conducted competition-binding assays with the same panel of WC RNA duplexes (referred to throughout as competition-processing assays). A representative gel displaying titration of ds22 to inhibit pri-mir-16-1 processing is shown in Figure 5(A), which yielded an IC_{50} of ~9 μ*M* (gels for all duplex inhibitors are shown in Supporting Information Figs. S7 and S8). As summarized in Table III, the trend toward lower IC_{50} values as dsRNA length increases, derived from the competition processing assays, follows a similar trend to that observed for $K_{d,app}$ in the EMSA experiments. Although the quantitative similarity between the IC_{50} and the $K_{d,app}$ values may be a coincidence, these results corroborate the finding that DGCR8 binds dsRNA in the size range of miRNA precursors well, with minimally higher efficiency for binding to longer RNA duplexes. To show that the trends observed were a result of duplex length, and not owing to the chosen nucleotide sequence, we also tested a 33-bp duplex with a randomized alternative sequence (ds33-alt) that, within experimental uncertainty, yielded the same IC_{50} as ds33 (Table III). Based on these results, we conclude that the EMSA assays report accurately the trends in DGCR8 binding to RNA in the context of the Microprocessor.

Binding to duplexes with flanking single strands

Drosha-processing assays have confirmed that the presence of an ssRNA–dsRNA junction approximately one turn of A-form helix removed from the Drosha cleavage site is required for processing.[20,21] As a result, it is common to draw schematics of the RNA-bound

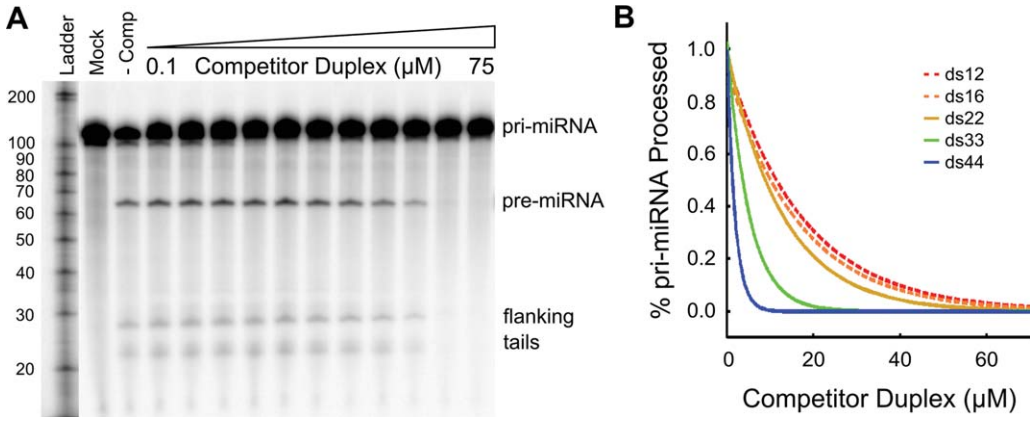

Figure 5
Competition-processing assays were used to corroborate the results of EMSA (Fig. 4) in a more biological context. (**A**) A representative gel using ds22 as the competitor is shown with the concentration of competitor increasing from left to right (triangle above gel). The leftmost lanes report a ladder, pri-mir-16-1 processing in the absence of transfected Microprocessor (Mock), and pri-mir-16-1 processed in the presence of transfected Microprocessor but the absence of any competitor duplex (-Comp). The positions of the pri-miRNA substrate and cleaved pre-miRNA and flanking tails are indicated to the right of the gels. (**B**) The corresponding fits to a single exponential decay model for all competitors are shown with solid lines (Table III, IC_{50} values); ds12 and ds16 estimated fits are displayed as dashed lines because these assays yielded only lower limits for IC_{50}. Representative competition-processing gels for all RNA constructs are shown in Supporting Information Figures S7 and S8.

Table III
Competition-Processing Assays Reporting Inhibition of pri-mir-16-1 Cleavage by the Microprocessor in the Presence of the Indicated Competitor Duplexes as IC_{50} values, with Uncertainties Based on Two Independent Replicates[a]

RNA construct	EMSAs (K_d)	Competition (IC_{50})
ds12	7.4 ± 0.9	>12
ds16	5.8 ± 0.8	>10
ds22	4.1 ± 0.5	8.9 ± 0.7
ds33	3.7 ± 0.3	4 ± 1
ds33-alt	N/D	4.7 ± 0.8
ds44	3.3 ± 0.2	1.3 ± 0.2

[a]EMSA-derived dissociation constants for DGCR8-Core binding to the same RNA duplexes from Table II are also provided for comparison.

Microprocessor with DGCR8 covering the ssRNA–dsRNA junction,[2,5,39,40] whereas Drosha engages the pri-miRNA cleavage site; however, direct binding of DGCR8 to the junction has never been demonstrated experimentally. To assess whether DGCR8 binding is sensitive to the presence of an ssRNA–dsRNA junction, we constructed a set of duplex RNA constructs, based on our ds16 duplex, which contain an additional 16 nucleotides of single-stranded tail(s) flanking the duplex (Fig. 6(A), secondary structures). The first construct contained both 5′- and 3′-flanking tails, matching those found in native pri-mir-16-1 (ds16 + native flanking). As the native pri-mir-16-1 sequence contains some WC complementarity in the flanking region, we also designed a construct with both 5′- and 3′-flanking tails in which the bottom strand is mutated to destroy all base-pair complementarity outside of the ds16 stem (ds16 + non-native flanking). Finally, we also annealed each of the three 32-mer flanking strands to their complementary 16-mer strands to generate the constructs with only a 5′-tail (ds16 + native flanking TS) or a 3′-tail (ds16 + native flanking BS; ds16 + non-native flanking BS). As a control, we also assayed DGCR8 interactions with 16-mer ssRNA (the top strand from the ds16 duplex) to test whether DGCR8-Core or DGCR8–dsRBD1 possesses an intrinsic affinity for ssRNA.

For DGCR8-Core, the EMSA-derived binding affinities for each of the five single-stranded flanking constructs

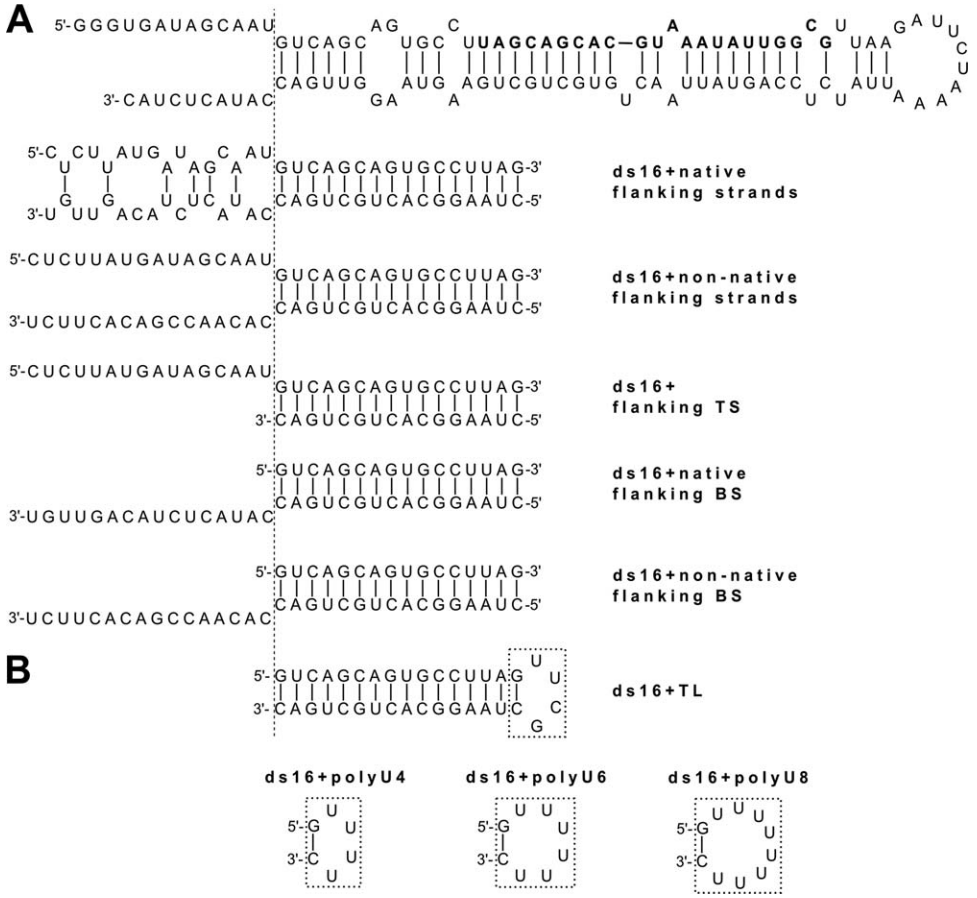

Figure 6

Secondary structures of (**A**) flanking and (**B**) terminal loop duplexes derived from pri-mir-16-1 (top). The various terminal loops are boxed to highlight the extent of the mutations.

Table IV
EMSA Best-Fit Parameters for DGCR8-Core Binding to pri-mir-16-1, Bearing the Indicated Mutations, with Uncertainties Based on Two Independent Replicates

RNA construct	DGCR8-Core (K_d, μM)
pri-mir-16-1-TL	1.0 ± 0.1
pri-mir-16-1-HS	2.70 ± 0.03
pri-mir-16-1-sec	1.2 ± 0.1

were more similar to the measured affinity for ds22 than to the measured affinity for ds16 (Table II; for gels, see Supporting Information Fig. S9), which suggests that the addition of an ssRNA–dsRNA junction does increase DGCR8-Core's binding affinity, albeit minimally. Significantly, the EMSA for DGCR8-Core interacting with the single-stranded 16-mer did show very weak binding ($K_{d,app} = 20$ μM, Table II; Supporting Information Fig. S10). As expected, the binding affinity of DGCR8–dsRBD1 across all flanking duplexes is much weaker than the affinity seen for DGCR8-Core (Table II; for gels, see Supporting Information Fig. S11) although quantitative assessment is difficult because saturation could not be reached. Taken together, our results support the possibility that DGCR8 interacts with single-stranded RNA in the context of the Microprocessor although it appears to be unlikely that DGCR8 is targeted to the ssRNA–dsRNA junction specifically.

Binding to RNA bearing terminal loop structures

Processing assays conducted by multiple groups have demonstrated that when the native terminal loops of pri-miRNA models are replaced by small terminal loops (especially thermostable UUCG tetraloops), Drosha processing is moderately to significantly diminished.[21,24,32,33] Intriguingly, the inhibition of pri-miRNA processing by binding of small molecules to the terminal loop has recently been demonstrated, implying that the terminal loop mediates important interactions with the Microprocessor.[41] Other data have led to the hypothesis that large, flexible terminal loops enhance RNA release and enzyme turnover after Drosha cleavage.[32,42] Given that we observed a weak interaction between DGCR8 and ssRNA in tails flanking ds16, we next tested for a direct impact on DGCR8 binding mediated by terminal loops. For this experiment, we designed another set of RNAs in which various terminal loops were used to close a 16-bp stem–loop secondary structure (Fig. 6(B), structures). This set included a stem–loop terminated by a thermally stable UUCG tetraloop (TL) and a series of three flexible polyU loops containing 4, 6, and 8 nucleotides (polyU4, polyU6, and polyU8, respectively).

The inspection of the EMSA results using these stem–loop RNAs as binding partners for DGCR8 reveals a slight increase in binding affinity for the large polyU octaloop construct, but no statistically significant change was found in affinity for either of the tetraloops (Table II; for gels, see Supporting Information Figs. S12 and S13). Motivated by this finding, we also designed pri-mir-16-1 variants in which the native terminal loop was replaced by the four experimental loop sequences described above (Fig. 2(B), secondary structures). Although pri-mir-16-1-TL has previously been shown to inhibit Drosha processing substantially,[24] it yielded a DGCR8-Core-binding constant that was almost identical to that seen for wild-type pri-mir-16-1 (Table IV; for a representative gel, see Supporting Information Fig. S14), suggesting that DGCR8 does not interact with the terminal loop strongly enough to impact function.

Intrigued by these findings, we next carried out *in vitro* Drosha-processing assays with the above described pri-mir-16-1 mutants to establish how well the binding affinities observed by EMSAs correlate with processing efficiency. For each construct, processing assays were performed under two different conditions: with the immunopurified Microprocessor (IP Micro) and with whole-cell extract generated from cells overexpressing both DGCR8 and Drosha (WCE). In all four cases, the same trend was observed irrespective of the method used as shown in Figure 7. As expected based on our prior experience,[24] the processing of the UUCG tetraloop mutant was significantly reduced. The extent of inhibition observed with the polyU4 loop was much less than for the pri-mir-16-1-TL construct, suggesting that the length of the loop alone is not the origin of the strong effect observed with the thermostable UUCG tetraloop construct. In fact, processing efficiency was diminished by the same amount with the constructs of polyU4, polyU6, and polyU8. Overall, the structure and nucleotide composition of the terminal loop is seen to have a significant impact on Drosha cleavage efficiency. Taken together with the EMSA studies, in which we observed that DGCR8 binding was largely insensitive to the presence or size of the terminal loop, we conclude that the impact of loop composition on processing cannot be attributed to direct recognition by DGCR8's dsRBDs.

Binding to pri-miRNA with reduced stem flexibility

Bioinformatic analysis has shown a tendency for pri-miRNAs to harbor non-WC helical defects near the Drosha cleavage site and approximately halfway between the Drosha and the Dicer cleavage sites, which we label the "hot spot" and secondary imperfection sites, respectively (Fig. 1).[22] Recently, we demonstrated that these helical defects enhance the local flexibility of the stem and that flexibility near the Drosha cleavage site in particular is necessary for high-efficiency pri-miRNA processing.[24] Motivated by these findings, we constructed this final set

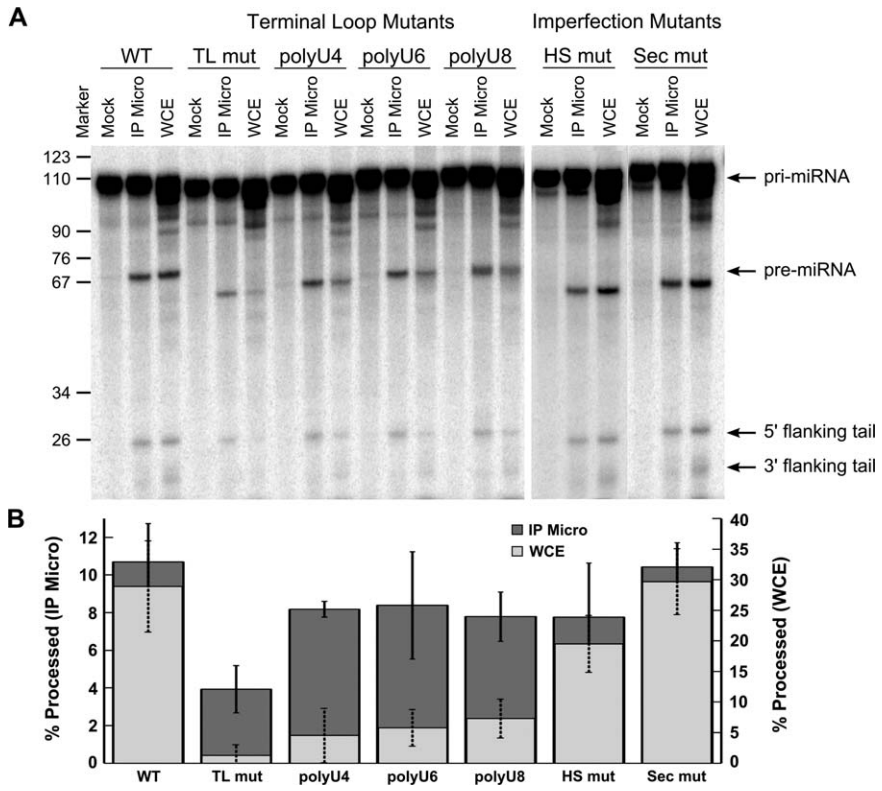

Figure 7

Drosha-processing assays show that the secondary structure of pri-miRNAs is an important determinant of Microprocessor cleavage efficiency *in vitro*. (**A**) Denaturing gels for the processing of native pri-mir-16-1 and its mutants: pri-mir-16-1-WT (WT), thermally stable tetraloop mutant (TL mut), polyU4 mutant (polyU4), polyU6 mutant (polyU6), polyU8 mutant (polyU8), "hot spot" mutant (HS mut), and secondary mutant (Sec mut). In each assay, lanes represent RNA exposed to FLAG beads with the addition of cell lysate that did not express FLAG-tagged proteins (Mock), exposed to the FLAG-tagged immunopurified Microprocessor (IP Micro), and exposed to whole-cell extract containing overexpressed Microprocessor (WCE). The positions of the pri-miRNA substrate, cleaved pre-miRNA, and flanking tails are indicated to the right of the gel. (**B**) The percentages of pri-miRNAs cleaved by the Microprocessor *in vitro* averaged over three independent experiments. Processing efficiencies are graphed for the immunopurified Microprocessor (left axis) and the whole-cell extract (right axis), with error bars to one standard deviation (for details, see Materials and Methods section).

of experiments to address whether DGCR8 binding is impacted by the presence of flexibility-inducing non-WC defects in the context of the dsRNA stems of pri-miRNA and our model duplexes. For this study, we used both our previously generated "hot spot" mutant in which the Drosha cleavage site of pri-mir-16-1 is mutated to be fully WC complementary (pri-mir-16-1-HS), and a new construct in which the secondary imperfection between the Drosha and the Dicer cleavage sites was also mutated to be fully WC complementary (pri-mir-16-1-sec). Secondary structures for both of these RNAs are shown in Figure 8(A). Similar to the EMSA results reported above for the panel of native pri-miRNAs, no significant difference in apparent dissociation constant for DGCR8-Core binding to these two stem-mutants was observed (Table IV; for representative gels, see Supporting Information Fig. S14).

To provide a more controlled assessment of the impact that these stem-stabilizing mutants may have on DGCR8 binding, we also assessed DGCR8 affinity in the context of otherwise ideal 22 bp duplexes (Fig. 8(B), secondary structures). The first duplex resembled the Drosha cut site (HS duplex), containing both the GA tandem mismatch and the A/C mismatch. For the secondary site, three duplexes were generated to assess the impact of combining symmetric and asymmetric defects: (1) miR:miR*, and hence named because of its similarity to the fully Drosha and Dicer processed native duplex, with both the A/A mismatch and the U-bulge; (2) dsAmis, containing only the A/A mismatch; and (3) dsUbulge, containing only the U-bulge.

For the dsUbulge duplex, the apparent DGCR8-binding affinity was decreased in comparison to the perfect ds22 duplex (Table II; for representative gels, see Supporting Information Fig. S15), most likely owing to the bending of the RNA duplex at the bulge. In contrast, no significant change in binding affinity was observed for the duplexes containing symmetric internal loops;

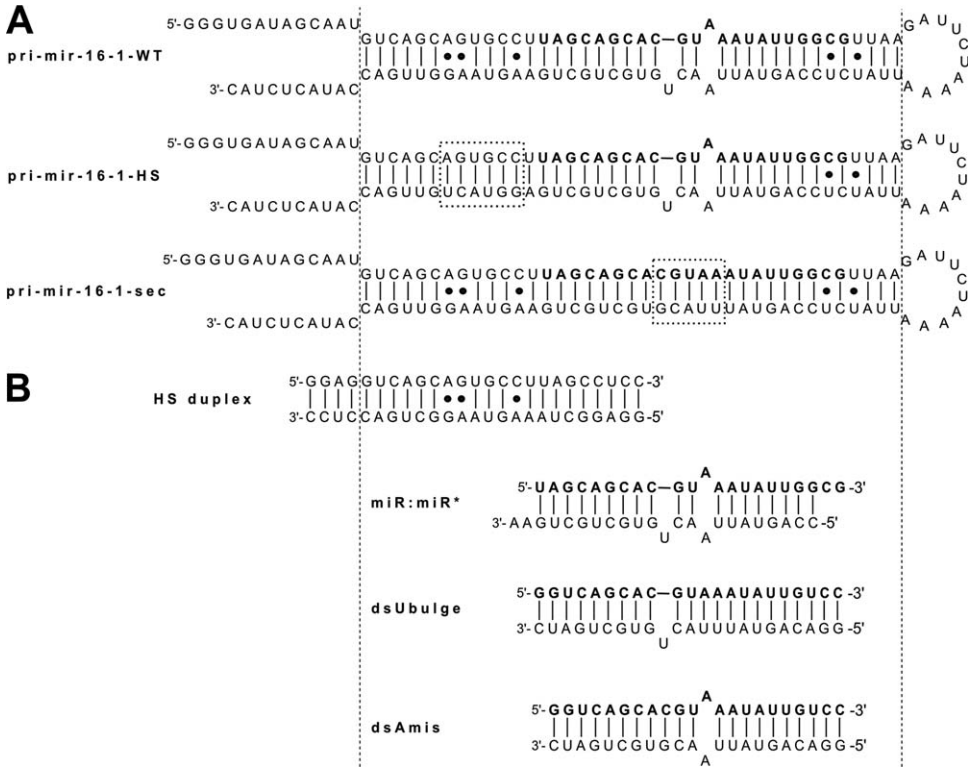

Figure 8

Secondary structures of constructs mimicking the imperfections found in pri-mir-16-1: (**A**) in the context of full-length pri-mir-16-1 and (**B**) in the context of short duplexes. The regions of mutation are boxed.

only a slight increase in affinity was seen for the dsAmis duplex. This result suggests that the mismatches in these RNAs do not significantly alter the average A-form geometry as it is common for symmetric internal loops.[43] These results are also similar to those recorded in our laboratory for TRBP interactions with similar duplexes.[44]

We have previously shown with immunopurified Microprocessor that Drosha processing is inhibited by the pri-mir-16-1-HS mutation,[24] which rigidifies the stem near the Drosha cut site. Continuing the *in vitro* processing assays first discussed for the stem–loop pri-miRNA mutants, this experiment was completed by assessing the impact of removing stem defects on Drosha cleavage efficiency, using both immunopurified Microprocessor and whole-cell extracts from cells overexpressing Drosha and DGCR8. Under both conditions, pri-mir-16-1-HS cleavage was significantly reduced as compared to wild-type pri-mir-16-1 (Fig. 7). In contrast, replacing the helical defects in the secondary site with WC base pairs had no effect on Drosha-processing efficiency under either IP or whole-cell extract conditions. Together with the EMSA assays, these results show that Drosha processing is sensitive to the presence of helical defects near the cut site, but that this effect cannot be attributed directly to DGCR8 binding.

RNA binding by DGCR8's heme-binding domain

Recently, the group of Feng Guo has introduced the hypothesis that a region of DGCR8 N-terminal to the "Core" element, which bears sequence homology to other proteins in the WW domain fold family, is essential for establishing high-affinity RNA binding by DGCR8 and, furthermore, that this activity is heme binding dependent.[37,45–47] Significantly, this hypothesis has recently been substantiated by the study of Roth *et al.*,[27] who reported enhanced dsRNA binding affinity measured by *in vitro* assays similar to those we utilize here. Therefore, we carried out binding assays using DGCR8-Core lengthened at its N-terminus to contain the heme-binding domain (DGCR8-HBD-Core; residues 276–720). Furthermore, the crystal structure of the heme-binding domain of DGCR8 (276–353) suggests that C352 binds to an iron-containing heme molecule through direct ligation of the iron by C352, which dimerizes DGCR8.[48] Therefore, we also performed binding assays with the DGCR8-HBD-Core construct mutated to convert the critical cysteine to alanine (C352A). Through these studies, we aim to evaluate whether the findings we have reported in this study are likely to be general or limited in scope to the context of the DGCR8-Core construct only.

Table V
EMSA Best-Fit Parameters for DGCR8-HBD-Core (with and without the C352A Mutation) Binding to pri-mir-16-1, pri-mir-16-1-TL, and ds44, with Uncertainties Based on Two Independent Replicates

	DGCR8-HBD-Core		DGCR8-HBD-Core (C352A)	
RNA construct	K_d (μM)	n	K_d (μM)	n
pri-mir-16-1	2.1 ± 0.1	4.1 ± 0.1	3.1 ± 0.1	3.0 ± 0.1
pri-mir-16-1-TL	2.2 ± 0.1	4.6 ± 0.1	3.1 ± 0.2	4.1 ± 0.2
ds44	4 ± 1	8 ± 1	4.7 ± 0.1	5 ± 1

As the binding constants summarized in Table V show, there is no statistically significant difference in DGCR8-Core and DGCR8-HBD-Core binding affinity for pri-mir-16-1, the pri-mir-16-1-TL mutant, or ds44 (for representative gels, see Supporting Information Figs. S16 and S17). The pri-mir-16-1-TL result is especially striking, because Quick-Cleveland *et al.*[47] have recently published the hypothesis that the HBD engages the open terminal loop of pri-miRNA as a necessary feature of high-affinity binding. It is noteworthy that our results contrast those of the Guo and Hennig groups, where an enhanced RNA-binding affinity is observed in the context of HBD-containing constructs that extend to the C-terminal residue of DGCR8 (276–773). This suggests that the disordered tail region between residues 720 and 773 is a necessary part of this affinity-switching mechanism. Also, we note that heme binding in the wild-type DGCR8-HBD-Core construct was confirmed by UV–visible spectroscopy as evidenced by the split Soret spectrum indicating a *bis*(thiolate) hyperporphyrin structure surrounding the iron center,[49] which disappeared upon the introduction of the C352A mutation (Supporting Information Fig. S18). Therefore, our results demonstrate that heme interaction with DGCR8 is not sufficient to enhance the RNA-binding affinity of DGCR8, suggesting that the heme-binding domain does not contribute directly to pri-miRNA binding.

Our binding results for the DGCR8-HBD-Core construct were surprising, because the introduction of a C352A mutation into the heme-binding domain has been previously shown to negatively impact pri-miRNA processing by Drosha[45] although outright deletion of the heme-binding domain has had contradictory impacts on pri-miRNA processing in the literature as well.[47] Therefore, we tested Drosha-processing efficiency in the background of the C352A mutant DGCR8, using pri-mir-16-1 as a substrate for consistency with the remainder of the study reported here. Additionally, we tested processing in the background of the pri-mir-16-1-TL and pri-mir-16-1-HS structural mutants. Consistent with the previous literature, we observe a decrease in processing efficiency for wild-type pri-mir-16-1 when the Microprocessor contains the DGCR8-C352A mutant construct (Fig. 9). Significantly, we observe a similar quantitative reduction in processing efficiency for both the pri-mir-16-1-TL and the pri-mir-16-1-HS mutants, indicating that regardless of functional role the heme-binding domain may be serving is independent from the mechanism that establishes the pri-miRNA structural preferences we have documented here.

DISCUSSION

It has been firmly established that DGCR8 and Drosha form the minimal complex required for efficient processing of pri-miRNAs during the first stage of miRNA maturation.[50] Interest in fully defining the mechanism of

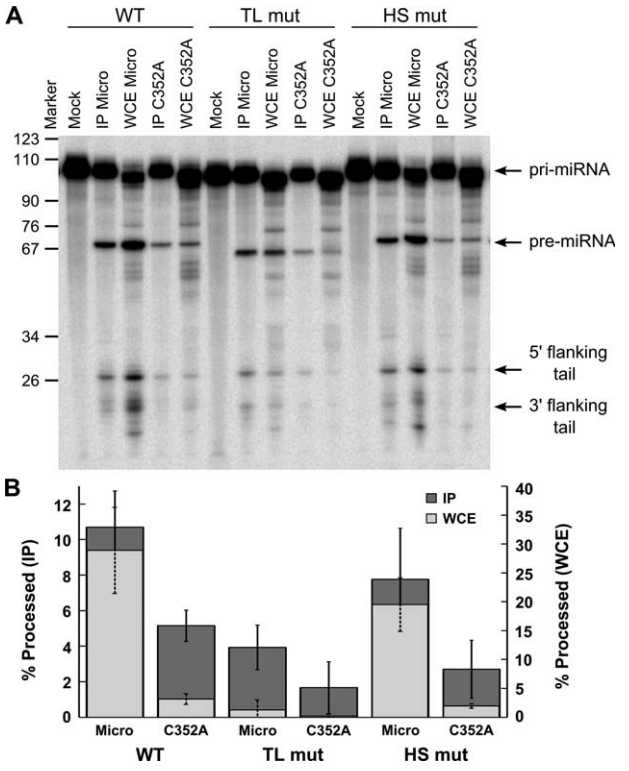

Figure 9
Drosha-processing assays show that the cysteine residue C352 is an important determinant of Microprocessor cleavage efficiency *in vitro*. (**A**) Denaturing gels for the processing of native pri-mir-16-1 and its mutants: pri-mir-16-1-WT (WT), thermostable tetraloop mutant (TL mut), and "hot spot" mutant (HS mut). In each assay, lanes represent RNA exposed to FLAG beads with the addition of cell lysate that did not express FLAG-tagged proteins (Mock), exposed to either the FLAG-tagged immunopurified Microprocessor or the whole-cell extract containing overexpressed Microprocessor for both the wild-type Microprocessor (IP Micro and WCE Micro, respectively) and the Microprocessor containing the C352A mutation in DGCR8 (IP C352A and WCE C352A, respectively). The positions of the pri-miRNA substrate, cleaved pre-miRNA, and flanking tails are indicated to the right of the gel. (**B**) The percentages of pri-miRNAs cleaved by the Microprocessor *in vitro* averaged over three independent experiments. Processing efficiencies are graphed for the immunopurified Microprocessor (left axis) and the whole-cell extract (right axis), with error bars to one standard deviation (for details, see Materials and Methods section).

cleavage by these proteins is high, because dysfunctional miRNA processing has been linked to the etiology of multiple diseases.[9] It is hypothesized that DGCR8 acts as a "molecular anchor" by forming a precleavage complex with pri-miRNA, promoting Drosha binding and establishing the appropriate cut site within the pri-miRNA.[21,51] Complicating matters, DGCR8 has been observed to interact with a plethora of RNAs in the nucleus in addition to pri-miRNAs,[52] suggesting that the rules for RNA selection and identification as pri-miRNA by DGCR8 may be more complex than previously appreciated. Therefore, understanding how the dsRBDs of DGCR8 collectively recognize their targets in the nucleus is a necessary step toward developing a molecular mechanism to describe pri-miRNA processing in the context of the miRNA maturation pathway.

Several dsRNA-binding proteins contain multiple copies of the dsRBD fold, suggesting that placing multiple dsRBDs in tandem promotes high-efficiency binding and possibly increased selectivity. One possible reason for a protein like DGCR8 to harbor two dsRBDs would be to increase binding affinity over that expected for a single dsRBD; yet our data show that this simple model is not sufficient to explain the structure of the protein. Although DGCR8-Core does bind each of the RNAs we investigated more strongly than DGCR8-dsRBD1 does, we have previously measured interactions between the isolated dsRBD from Dicer and the same panel of dsRNAs, reporting binding affinities that are essentially indistinguishable from the DGCR8-Core affinities reported here.[53] Thus, DGCR8 could have achieved the observed dual-dsRBD affinities with a single dsRBD of different sequence. As suggested by Faller *et al.*[37] and by the high Hill coefficients from the EMSAs in this study, an alternative explanation is that DGCR8-Core binds dsRNA cooperatively, whereas the isolated dsRBDs are capable of doing so. The EMSA results in this study demonstrate that the isolated N-terminal dsRBD of DGCR8 binds inefficiently to short duplexes (<22 bp) or to duplexes possessing significant single-stranded character. In contrast, DGCR8-Core shows marginal changes in $K_{d,app}$ across the duplex length range tested and is more resilient to the incorporation of ssRNA into the duplex. This suggests that the arrangement of two dsRBDs in DGCR8-Core may have evolved to increase DGCR8's resilience to the structural diversity commonly encountered across the set of hundreds of pri-miRNAs it must assist in processing. Overall, our binding results are highly consistent with those of Roth *et al.*[27] while providing broader coverage of RNA structural motifs that strengthens our confidence in the general nature of our collective findings.

The current model for Drosha substrate selection by DGCR8 suggests that the identification of pri-miRNAs is achieved, in part, by direct interactions between the DGCR8 and the ssRNA–dsRNA junction at the base of the pri-miRNA stem.[2,40] Crystallography of the unbound DGCR8-Core particle, supported by FRET measurements, has also led to the hypothesis that DGCR8 wraps the pri-miRNA stem around its two dsRBDs.[25] The observed formation of a stable interface between the two dsRBDs of DGCR8-Core in the unbound state is unique and contrasts with the solution structures of the dual-dsRBD proteins PKR[54] and TRBP,[55] and yet extensive NMR spectroscopic data support the presence of this interface in solution,[27,56] lending credence to the RNA-wrapping model. However, the proposals that DGCR8-Core interacts with the ssRNA–dsRNA junction and that it wraps the RNA stem around itself in the bound state are not mutually exclusive as the wrapping model can still place the ssRNA–dsRNA junction in contact with DGCR8 for reasonable stem lengths (e.g., see the model in Fig. 1). Evidence in support of both elements of this model has been provided by Drosha-processing assays, which show reduced efficiency when the ssRNA–dsRNA junction or flexible sites internal to the stem are eliminated.[20,21,24,33] The results of this study confirm that the dsRBD-containing region of DGCR8 is capable of high affinity binding to dsRNA, consistent with it being the minimal region necessary for the recruitment of RNA to the Microprocessor; but binding of dsRNA to DGCR8-Core is not enhanced by the the addition of single-stranded flanking regions, or by the presence of a hairpin-forming stem–loop. Furthermore, the elimination of the two regions of enhanced flexibility within the stem did not inhibit DGCR8-Core binding; nor did the elimination of secondary site flexibility inhibit *in vitro* processing. Therefore, we conclude that interactions mediated by DGCR8-Core alone cannot be responsible for generating the previously observed criteria for efficient cleavage of RNAs recruited to the Microprocessor complex.

Given that the "Core"-binding region of DGCR8 is not responsible for the recognition of specific structural features within pri-miRNAs, identifying the molecular mechanism of specific target recognition remains a high priority. To this end, we investigated the previously hypothesized role of DGCR8's heme-binding region[47] in target RNA selection. Our data support the conclusion that the heme-binding domain does not contribute to the recognition of specific structural features within pri-miRNA targets. The previous studies have shown an increase in RNA-binding affinity for full-length DGCR8 (less the nuclear localization signal) in comparison to the "Core"-binding region; however, our data suggest that the heme-binding region is not responsible for this change, at least in the context of the DGCR8-HBD-Core construct. This conclusion is further supported by previous reports of efficient *in vitro* processing of pri-miRNAs using Microprocessor reconstituted with DGCR8 that is missing the heme-binding region.[37,38,47]

At first glance, the collective findings reported here seem negative—no strong connection is observed

between DGCR8-Core-binding affinity and the inclusion of any structural features in the dsRNA targets. This result is unexpected, because DGCR8-Core matches well to the minimal fragment of DGCR8 that it is necessary to promote *in vitro* pri-miRNA processing, suggesting that the job of selecting pri-miRNAs from the diverse cellular RNA pool may be dependent on a region of DGCR8 not necessary for efficient *in vitro* processing. Recent studies suggest that this latter point has merit.[47] However, taking the converse view of these data suggests a new hypothesis. We propose that the unique spatial arrangement of two dsRBDs within DGCR8-Core promotes efficient cleavage for a broad set of substrates by disconnecting recruitment efficiency from the vagaries of the unique structure features seen in individual pri-miRNA substrates and, furthermore, that this insensitivity is necessary to support DGCR8's Drosha-independent functions. It appears to be likely that DGCR8 binds to nearly all of the dsRNAs it encounters in the nucleus and that the identification of some RNAs as pri-miRNAs may be a function of Drosha itself.

ACKNOWLEDGMENTS

The authors thank Roderico Acevedo for assistance with EMSA assays and Philip Bevilacqua for helpful discussion while developing the experimental protocols. The authors also thank Nick Lanz and Jamie Arnold for help in molecular biology protocols. Finally, they thank the Huck Institutes for the Life Sciences Shared Fermentation Facility for providing access to cell culture equipment.

REFERENCES

1. Zangi L, Lui KO, von Gise A, Ma Q, Ebina W, Ptaszek LM, Später D, Xu H, Tabebordbar M, Gorbatov R, Sena B, Nahrendorf M, Briscoe DM, Li RA, Wagers AJ, Rossi DJ, Pu WT, Chien KR. Modified mRNA directs the fate of heart progenitor cells and induces vascular regeneration after myocardial infarction. Nat Biotechnol 2013;31:898–907.
2. Li Z, Rana TM. Therapeutic targeting of microRNAs: current status and future challenges. Nat Rev Drug Discov 2014;13:622–638.
3. Bora RS, Gupta D, Mukkur TK, Saini KS. RNA interference therapeutics for cancer: challenges and opportunities (review). Mol Med Rep 2012;6:9–15.
4. Castel SE, Martienssen RA. RNA interference in the nucleus: roles for small RNAs in transcription, epigenetics and beyond. Nat Rev Genet 2013;14:100–112.
5. Ha M, Kim VN. Regulation of microRNA biogenesis. Nat Rev Mol Cell Biol 2014;15:509–524.
6. Ding Y, Tang Y, Kwok CK, Zhang Y, Bevilacqua PC, Assmann SM. In vivo genome-wide profiling of RNA secondary structure reveals novel regulatory features. Nature 2014;505:696–700.
7. Rouskin S, Zubradt M, Washietl S, Kellis M, Weissman JS. Genome-wide probing of RNA structure reveals active unfolding of mRNA structures in vivo. Nature 2014;505:701–705.
8. Talkish J, May G, Lin Y, Woolford JL Jr, McManus CJ. Mod-seq: high-throughput sequencing for chemical probing of RNA structure. RNA 2014;20:713–720.
9. van Kouwenhove M, Kedde M, Agami R. MicroRNA regulation by RNA-binding proteins and its implications for cancer. Nat Rev Cancer 2011;11:644–656.
10. Tian B, Bevilacqua PC, Diegelman-Parente A, Mathews MB. The double-stranded-RNA-binding motif: interference and much more. Nat Rev Mol Cell Biol 2004;5:1013–1023.
11. Masliah G, Barraud P, Allain FH. RNA recognition by double-stranded RNA binding domains: a matter of shape and sequence. Cell Mol Life Sci 2013;70:1875–1895.
12. Tian B, Mathews MB. Phylogenetics and functions of the double-stranded RNA-binding motif: a genomic survey. Prog Nucleic Acid Res Mol Biol 2003;74:123–158.
13. Nagai K. RNA-protein complexes. Curr Opin Struct Biol 1996;6:53–61.
14. Ryter JM, Schultz SC. Molecular basis of double-stranded RNA-protein interactions: structure of a dsRNA-binding domain complexed with dsRNA. EMBO J 1998;17:7505–7513.
15. Ramos A, Grünert S, Adams J, Micklem DR, Proctor MR, Freund S, Bycroft M, St Johnston D, Varani G. RNA recognition by a Staufen double-stranded RNA-binding domain. EMBO J 2000; 19:997–1009.
16. Blaszczyk J, Gan J, Tropea JE, Court DL, Waugh DS, Ji X. Noncatalytic assembly of ribonuclease III with double-stranded RNA. Structure 2004;12:457–466.
17. Yang SW, Chen HY, Yang J, Machida S, Chua NH, Yuan YA. Structure of arabidopsis HYPONASTIC LEAVES1 and its molecular implications for miRNA processing. Structure 2010;18:594–605.
18. Wang Z, Hartman E, Roy K, Chanfreau G, Feigon J. Structure of a yeast RNase III dsRBD complex with a noncanonical RNA substrate provides new insights into binding specificity of dsRBDs. Structure 2011;19:999–1010.
19. Stefl R, Oberstrass FC, Hood JL, Jourdan M, Zimmermann M, Skrisovska L, Maris C, Peng L, Hofr C, Emeson RB, Allain FH. The solution structure of the adar2 dsRBM-RNA complex reveals a sequence-specific readout of the minor groove. Cell 2010;143:225–237.
20. Zeng Y, Cullen BR. Efficient processing of primary microRNA hairpins by Drosha requires flanking nonstructured RNA sequences. J Biol Chem 2005;280:27595–27603.
21. Han JJ, Lee Y, Yeom KH, Nam JW, Heo I, Rhee JK, Sohn SY, Cho YJ, Zhang BT, Kim VN. Molecular basis for the recognition of primary microRNAs by the Drosha-dgcr8 complex. Cell 2006;125:887–901.
22. Warf MB, Johnson WE, Bass BL. Improved annotation of *C. elegans* microRNAs by deep sequencing reveals structures associated with processing by Drosha and dicer. RNA 2011;17:563–577.
23. Sperber H, Beem A, Shannon S, Jones R, Banik P, Chen Y, Ku S, Varani G, Yao S, Ruohola-Baker H. miRNA sensitivity to Drosha levels correlates with pre-miRNA secondary structure. RNA 2014;20:621–631.
24. Quarles KA, Sahu D, Havens MA, Forsyth ER, Wostenberg C, Hastings ML, Showalter SA. Ensemble analysis of primary microRNA structure reveals an extensive capacity to deform near the Drosha cleavage site. Biochemistry 2013;52:795–807.
25. Sohn SY, Bae WJ, Kim JJ, Yeom KH, Kim VN, Cho Y. Crystal structure of human dgcr8 core. Nat Struct Mol Biol 2007;14:847–853.
26. Wostenberg C, Noid WG, Showalter SA. MD simulations of the dsRBP dgcr8 reveal correlated motions that may aid pri-miRNA binding. Biophys J 2010;99:248–256.
27. Roth BM, Ishimaru D, Hennig M. The core microprocessor component DiGeorge syndrome critical region 8 (dgcr8) is a nonspecific RNA-binding protein. J Biol Chem 2013;288:26785–26799.
28. Starega-Roslan J, Krol J, Koscianska E, Kozlowski P, Szlachcic WJ, Sobczak K, Krzyzosiak WJ. Structural basis of microRNA length variety. Nucleic Acids Res 2011;39:257–268.
29. Wostenberg C, Quarles KA, Showalter SA. Dynamic origins of differential RNA binding function in two dsRBDs from the miRNA "microprocessor" complex. Biochemistry 2010;49:10728–10736.

30. Havens MA, Reich AA, Duelli DM, Hastings ML. Biogenesis of mammalian microRNAs by a non-canonical processing pathway. Nucleic Acids Res 2012;40:4626–4640.
31. Burke JM, Kelenis DP, Kincaid RP, Sullivan CS. A central role for the primary microRNA stem in guiding the position and efficiency of Drosha processing of a viral pri-miRNA. RNA 2014;20:1068–1077.
32. Zhang X, Zeng Y. The terminal loop region controls microRNA processing by Drosha and dicer. Nucleic Acids Res 2010;38:7689–7697.
33. Zeng Y, Cullen BR. Sequence requirements for micro RNA processing and function in human cells. RNA 2003;9:112–123.
34. Fu Q, Yuan YA. Structural insights into RISC assembly facilitated by dsRNA-binding domains of human RNA helicase a (dhx9). Nucleic Acids Res 2013;41:3457–3470.
35. Bevilacqua PC, Cech TR. Minor-groove recognition of double-stranded RNA by the double-stranded RNA-binding domain from the RNA-activated protein kinase PKR. Biochemistry 1996;35:9983–9994.
36. Parker GS, Maity TS, Bass BL. dsRNA binding properties of RDE-4 and TRBP reflect their distinct roles in RNAi. J Mol Biol 2008;384:967–979.
37. Faller M, Toso D, Matsunaga M, Atanasov I, Senturia R, Chen Y, Zhou ZH, Guo F. Dgcr8 recognizes primary transcripts of microRNAs through highly cooperative binding and formation of higher-order structures. RNA 2010;16:1570–1583.
38. Yeom KH, Lee Y, Han JJ, Suh MR, Kim VN. Characterization of dgcr8/pasha, the essential cofactor for Drosha in primary miRNA processing. Nucleic Acids Res 2006;34:4622–4629.
39. Ameres SL, Zamore PD. Diversifying microRNA sequence and function. Nat Rev Mol Cell Biol 2013;14:475–488.
40. Rottiers V, Näär AM. MicroRNAs in metabolism and metabolic disorders. Nat Rev Mol Cell Biol 2012;13:239–250.
41. Diaz JP, Chirayil R, Chirayil S, Tom M, Head KJ, Luebke KJ. Association of a peptoid ligand with the apical loop of pri-miR-21 inhibits cleavage by Drosha. RNA 2014;20:528–539.
42. Zeng Y, Yi R, Cullen BR. Recognition and cleavage of primary microRNA precursors by the nuclear processing enzyme Drosha. EMBO J 2005;24:138–148.
43. Bevilacqua PC, George CX, Samuel CE, Cech TR. Binding of the protein kinase PKR to RNAs with secondary structure defects: role of the tandem a-G mismatch and noncontiguous helixes. Biochemistry 1998;37:6303–6316.
44. Acevedo R, Orench-Rivera N, Quarles KA, Showalter SA. Helical defects in MicroRNA influence protein binding by TAR RNA binding protein. PLoS One 2015;10:e0116749.
45. Faller M, Matsunaga M, Yin S, Loo JA, Guo F. Heme is involved in microRNA processing. Nat Struct Mol Biol 2007;14:23–29.
46. Barr I, Smith AT, Senturia R, Chen Y, Scheidemantle BD, Burstyn JN, Guo F. DiGeorge critical region 8 (dgcr8) is a double-cysteine-ligated heme protein. J Biol Chem 2011;286:16716–16725.
47. Quick-Cleveland J, Jacob JP, Weitz SH, Shoffner G, Senturia R, Guo F. The dgcr8 RNA-binding heme domain recognizes primary microRNAs by clamping the hairpin. Cell Rep 2014;7:1994–2005.
48. Senturia R, Faller M, Yin S, Loo JA, Cascio D, Sawaya MR, Hwang D, Clubb RT, Guo F. Structure of the dimerization domain of DiGeorge critical region 8. Protein Sci 2010;19:1354–1365.
49. Dawson JH, Sono M. Cytochrome P-450 and chloroperoxidase—thiolate-ligated heme enzymes—spectroscopic determination of their active-site structures and mechanistic implications of thiolate ligation. Chem Rev 1987;87:1255–1276.
50. Gregory RI, Yan KP, Amuthan G, Chendrimada T, Doratotaj B, Cooch N, Shiekhattar R. The microprocessor complex mediates the genesis of microRNAs. Nature 2004;432:235–240.
51. Nicholson AW. Ribonuclease III mechanisms of double-stranded RNA cleavage. Wiley Interdiscip Rev RNA 2014;5:31–48.
52. Macias S, Plass M, Stajuda A, Michlewski G, Eyras E, Cáceres JF. Dgcr8 HITS-CLIP reveals novel functions for the microprocessor. Nat Struct Mol Biol 2012;19:760–766.
53. Wostenberg C, Lary JW, Sahu D, Acevedo R, Quarles KA, Cole JL, Showalter SA. The role of human Dicer-dsRBD in processing small regulatory RNAs. PLoS One 2012;7:e51829.
54. Ucci JW, Kobayashi Y, Choi G, Alexandrescu AT, Cole JL. Mechanism of interaction of the double-stranded RNA (dsRNA) binding domain of protein kinase R with short dsRNA sequences. Biochemistry 2007;46:55–65.
55. Benoit MP, Plevin MJ. Backbone resonance assignments of the micro-RNA precursor binding region of human TRBP. Biomol NMR Assign 2013;7:229–233.
56. Roth BM Hennig M. Backbone ^{1}HN, ^{13}C, and ^{15}N resonance assignments of the tandem RNA-binding domains of human dgcr8. Biomol NMR Assign 2013;7:183–186.